Proceedings of the
9th Graz Brain-Computer Interface Conference 2024
10.3217/978-3-99161-014-4-004

OPTIMIZING TIME-VARYING AUTOREGRESSIVE MODELS FOR BCI APPLICATIONS

Kyriaki Kostoglou[1], Gernot Müller Putz[1,2]

[1] Institute of Neural Engineering, Graz University of Technology, Graz, Austria
[2] BioTechMed Graz, Graz, Austria

E-mail: kkostoglou@tugraz.at

ABSTRACT: Monitoring the spectral characteristics of brain signals can provide insights into the underlying processes responsible for their generation. In brain-computer interface (BCI) applications, this is relatively important in decoding neural activity as it can provide a means to differentiate between various tasks or mental states. To capture spectral variations, herein, we focus on time-varying autoregressive models (TVAR). We introduce a framework designed to efficiently optimize and apply these models to multi-trial and multi-channel data, including electroencephalography (EEG) signals. Our approach was validated using EEG data from motor imagery tasks.

INTRODUCTION

Time-varying autoregressive (TVAR) models are widely utilized in brain-computer interface (BCI) research, serving various purposes including time-varying power spectral density estimation to analyze shifts in brain dynamics [1], [2], [3], as well as feature extraction crucial for online BCI applications [4], [5], [6], [7], [8], [9], [10]. AR models, known for their ability to capture prominent frequency components in the signals, provide a powerful tool for brain activity analysis. The integration of TV estimation techniques further enhances their effectiveness, enabling real-time monitoring of temporal variations in these components.

The central focus of these models revolves around the autoregressive (AR) coefficients, which play a fundamental role in shaping the power spectrum characteristics of the analyzed signal. By segmenting the data into overlapping quasi-stationary windows, one can monitor the temporal evolution of these coefficients. This approach facilitates the detection of changes in the signal dynamics associated with alterations in the user's cognitive processes or task-related activities. The estimated coefficients can subsequently be used for classification purposes. Alternatively, to streamline the process and eliminate the need for data segmentation, recursive techniques such as Recursive Least Squares (RLS) and Kalman Filtering (KF) can be employed. These methods provide at each time sample an estimate of the AR coefficients without the necessity of dividing the data into separate windows, which typically results in increased processing time.

Despite the widespread application of TVAR models, limited studies have focused on optimizing their use, particularly in the context of feature extraction and classification within BCIs. Many studies resort to windowing approaches due to the absence of clear guidelines on employing recursive techniques. They also rely on predefined model structures derived from previous literature, potentially compromising model performance. One of the primary questions that we will try to answer here is how to effectively tune and integrate these models into multi-channel signals and apply them to unseen datasets and online BCI scenarios. Schlögl et al. [4], Pfurtscheller et al. [5] and Brunner et al. [7] were among the first to provide a comprehensive framework on TVAR models for single-trial electroencephalography (EEG) classification. They proposed methods to optimally tune the model hyperparameters, as well as strategies for integrating recursive techniques, as these techniques also impact the estimation results.

Inspired from [4], [5] and [7], we herein, explore further the application of these models and we present a concise methodological approach that can be readily implemented and extended to other TVAR model variants such as TV multivariate AR models [11], [12] and root tracking techniques [13], [14] for offline and online BCI applications. We furthermore propose the incorporation of an additional feature derived from the tracking process, in addition to the commonly employed TVAR coefficients, for classification purposes. This recommendation arises from our observation of increased accuracy when incorporating this additional feature. To validate our approach, we used a publicly available EEG dataset that consists of four different motor imagery tasks [7], [15].

MATERIALS AND METHODS

Time-varying Autoregressive Model (TVAR): In a TVAR model, the current value of a time-series $\boldsymbol{y}$ is expressed as a linear combination of its past values [16],

$$y(n) = \sum_{k=1}^{p} a_k(n) y(n-k) + e(n), \qquad \boldsymbol{e} \sim N(0, R) \quad (1)$$

where $\boldsymbol{a}(n) = [a_1(n) \dots . a_p(n)]^T$ are the AR coefficients at time point n, p denotes the model order which specifies the number of past lags considered and $e(n)$ is zero mean, white gaussian noise with variance R.

Published by
Verlag der Technischen Universität Graz

10.3217/978-3-99161-014-4-004

In practical terms, Eq. 1 assumes that the analyzed signal is the output of a TV filter driven by white gaussian noise. The characteristics of the filter as well as its temporal variations are captured by the TVAR coefficients.

Kalman Filter (KF): One common technique used to estimate and track the coefficients of Eq. 1 is the KF. The KF models the temporal evolution of the AR coefficients as a random walk driven by white gaussian noise (also known as process noise) with variance Q,

$$\boldsymbol{a}(n) = \boldsymbol{a}(n-1) + \boldsymbol{w}(n), \qquad \boldsymbol{w} \sim \boldsymbol{N}(0, Q) \quad (2)$$

Q essentially dictates the magnitude of the expected coefficient variations. Eq. 1 can thus be expressed as,

$$y(n) = \boldsymbol{a}^T(n)\boldsymbol{\varphi}(n) + e(n), \quad \boldsymbol{e} \sim N(0, R) \quad (3)$$

where $\boldsymbol{\varphi}(n) = [y(n-1) \dots y(n-k)]^T$ is the regressor vector, at time point n, containing past lags of the time-series. Using the AR state-space representation of Eqs. 2-3, the KF algorithm can be employed to estimate the AR coefficients (i.e., state variables) at each time point,

$$\hat{e}(n) = y(n) - \boldsymbol{\varphi}^{\boldsymbol{T}}(n)\hat{\boldsymbol{a}}(n-1) \quad (4)$$

$$\boldsymbol{K}(n) = \frac{\boldsymbol{P}(n-1)\boldsymbol{\varphi}(n)}{R + \boldsymbol{\varphi}^{\boldsymbol{T}}(n)\boldsymbol{P}(n-1)\boldsymbol{\varphi}(n)} \quad (5)$$

$$\boldsymbol{P}(n) = \boldsymbol{P}(n-1) + Q\boldsymbol{I} - \boldsymbol{K}(n)\boldsymbol{\varphi}^{\boldsymbol{T}}(n)\boldsymbol{P}(n-1) \quad (6)$$

$$\hat{\boldsymbol{a}}(n) = \hat{\boldsymbol{a}}(n-1) + \boldsymbol{K}(n)\hat{e}(n) \quad (7)$$

where $\hat{e}(n)$ is the one-step ahead prediction error, $\hat{\boldsymbol{a}}(n)$ are the tracked TVAR coefficients and $\boldsymbol{K}(n)$ is the Kalman gain matrix which minimizes the a posteriori error covariance $\boldsymbol{P}(n)$. The combination of KF and AR models will be referred to, herein, as KF-TVAR.

KF-TVAR hyperparameters: As indicated in [4], the performance of the KF-TVAR approach depends on several factors. Here, we focus on the following model hyperparameters:

- The AR model order p as it impacts the representation of the captured underlying dynamics.
- The values R and Q of the measurement and process noise, respectively. Q defines the magnitude of the AR coefficient variations, whereas R represents the variance of the underlying noise.
- The initial value of the covariance matrix $\boldsymbol{P}$. A common practice is to set the initial covariance matrix $\boldsymbol{P}(0)$ to a diagonal matrix $\boldsymbol{P}(0) = P_0\boldsymbol{I}$ where P_0 is typically assigned a large value. This choice determines the initial uncertainty associated with the estimated coefficients and affects the early KF tracking behavior.
- The initial coefficient estimates $\hat{\boldsymbol{a}}(0)$. If the initial coefficients approximate the true values at the analyzed time point, the KF-TVAR model is more likely to quickly converge or adapt to changes in the AR coefficients over time.

Other factors influencing the KF-TVAR performance: In addition to the aforementioned hyperparameters, the performance of the KF-TVAR model can be influenced by various signal preprocessing steps. For instance, the choice of sampling rate has been demonstrated to impact the KF-TVAR tracking accuracy [17]. Here, we focus on spatial filtering methods and particularly on the common average reference (CAR) filtering technique which is widely applied in BCI research.

Adapting and tuning the KF-TVAR method on multi-channel and multi-trial signals: BCI systems typically rely on multi-channel signals. These systems are built upon a training dataset to establish associations between the features and the desired target tasks. Once adequately trained, they can make predictions or classifications on unseen data. This study focuses on extracting TVAR coefficients as key features for classification purposes. Since the data includes multi-channel and, typically, multi-trial signals we propose a two-step approach. The first step involves optimizing the KF hyperparameters, namely $R, Q, P_0, \hat{\boldsymbol{a}}^T(0)$ in a data-driven manner for varying AR model orders. The second step includes extraction of the TVAR coefficients and classification. During this step, the optimal AR model order is selected based on cross-validation (CV). Our proposed approach can be summarized as follows,

Step 1) Select the first, in chronological order, trial from each class of the training set.

Step 2) For an ascending model order p (e.g., $p = 1 \dots 12$) , apply the KF-TVAR approach to each channel and tune the model hyperparameters $X_p = [R, Q, P_0, \hat{\boldsymbol{a}}^T(0)]$ using a genetic algorithm (GA) [18] or any other global optimization technique. As objective function, based also on the work of Schlögl et al. [4], we propose the average normalized mean squared error (NMSE) within the selected trials defined as,

$$J(X_p) = \frac{1}{C}\sum_{k=1}^{C}\frac{\|\hat{e}_k\|_2^2}{\|y_k\|_2^2} \quad (8)$$

where C is the number of classes (and therefore trials used for model optimization), $\hat{\boldsymbol{e}}_k$ is the a priori error of Eq. 4 and $\boldsymbol{y}_k$ the corresponding channel signal belonging to the k^{th} class/trial. The optimization process can be performed separately for each channel, yielding different sets of hyperparameters. However, an alternative strategy involves averaging Eq. 8 across all channels to obtain a unified set of hyperparameters.

Step 3) For each model order p, use the obtained hyperparameter set/sets X_p and apply the KF-TVAR technique to all subsequent training trials to extract the TVAR coefficients from each channel. Furthermore, as an additional feature we propose the TV trace of the covariance matrix $\boldsymbol{P}(n)$ (Eq. 6). Within each trial, the feature vector at each time point consists of the concatenated AR coefficients and KF covariance traces from all channels resulting into a vector of dimension $M \cdot p + M$, where M is the number of channels. If the covariance trace is excluded, the vector's dimensionality becomes $M \cdot p$.

Step 4) For each model order p, employ a machine learning algorithm to map the relationship between TVAR coefficients and the various target classes. The optimal AR order p_{opt} can be selected through cross-validation within the training set. Note that the same AR

Published by
Verlag der Technischen Universität Graz

 10.3217/978-3-99161-014-4-004

model order is applied across all channels.

Step 5) Use p_{opt} and the set of hyperparameters $X_{p_{opt}}$ obtained in step 2 on a new dataset or for online tracking.

Data: The proposed KF-TVAR methodology was applied to dataset 2a of the BCI competition IV (https://www.bbci.de/competition/iv/) [15]. This dataset consists of EEG recordings from nine subjects during four cue-based motor imagery tasks, namely movement imagination of the tongue, the left and the right hand and both feet. The recordings were obtained on two different days. Each session consisted of 72 trials from each class. At the start of each session, a recording lasting approximately 5 minutes was conducted to assess the influence of the electrooculogram (EOG). The EEG data comprised 22 channels, sampled at a rate of 200 Hz, and bandpass-filtered within the range of 0.5 to 100 Hz.

Signal preprocessing: All the analysis was conducted in Matlab (The Mathworks Inc.). The EOG from the initial 5-minute recordings was utilized to perform linear regression on the EEG. The coefficients obtained from this regression were then applied to remove the influence of EOG artifacts from all subsequent EEG recordings during the session. The EEG signals were then resampled to 64Hz and were temporally aligned around the cue onset, with a window spanning from -2 to 7 seconds. We analyzed the data with and without CAR filtering.

Applying the KF-TVAR methodology: Initially, the KF-TVAR optimization was employed to each channel separately (single-channel optimization) and we extracted as features for classification only the TV-AR coefficients. To examine the effect of the initial coefficient estimates $\hat{\boldsymbol{a}}(0)$, we first set them to 0 and then we allowed the GA to optimize them. We then included the TV trace of the $\boldsymbol{P}(n)$ matrix as an extra feature for classification. Finally, we examined the approach of obtaining one set of KF-TVAR hyperparameters for all channels (multi-channel optimization). The different approaches were categorized as follows:

Single-channel optimization and feature extraction:

For each channel and each investigated model order, the GA provided an optimal hyperparameter set X_p by minimizing Eq. 8. These values were then used to extract KF-TVAR features. We examined the following scenarios,

- **sC0W0:** $\hat{\boldsymbol{a}}(0)$ set to 0, TV-AR coefficients extracted for classification.
- **sC0W1:** $\hat{\boldsymbol{a}}(0)$ optimized by the GA, TV-AR coefficients extracted for classification.
- **sC1W0:** CAR rereferencing, $\hat{\boldsymbol{a}}(0)$ set to 0, TV-AR coefficients extracted for classification.
- **sC1W1:** CAR rereferencing, $\hat{\boldsymbol{a}}(0)$ optimized by the GA, TV-AR coefficients extracted for classification.
- **sC1W1$^+$:** CAR rereferencing, $\hat{\boldsymbol{a}}(0)$ optimized by the GA, both TV-AR coefficients and TV $\boldsymbol{P}(n)$ trace extracted for classification.

Multi-channel optimization and feature extraction:

For each model order, the GA provided a unified set of hyperparameters X_p by minimizing the average of Eq. 8 across all channels. The scenarios we examined are summarized below.

- **mC1W1:** CAR rereferencing, $\hat{\boldsymbol{a}}(0)$ optimized by the GA, TVAR coefficients extracted for classification.
- **mC1W1$^+$:** CAR rereferencing, $\hat{\boldsymbol{a}}(0)$ optimized by the GA, both TVAR coefficients and TV $\boldsymbol{P}(n)$ trace extracted for classification.

Finally, for both single-channel and multi-channel approaches, the optimal model order p_{opt} was selected based on the CV performance. Subsequently, the KF-TVAR X_p set provided by the GA, corresponding to p_{opt}, (i.e., $X_{p_{opt}}$) was used to estimate KF-TVAR features.

Classification: By applying the KF-TVAR methodology within each trial of the first session (Session 1) we obtained features at each time sample (see Step 3). Since all trials were aligned to the cue onset, we utilized a sample-by-sample classification approach wherein a shrinkage linear discriminant analysis (sLDA) model was trained on each individual time sample relative to the cue onset (covariance shrinkage was applied using the Matlab toolbox covShrinkage [19]). Additionally, we employed a trial-based 10x1 fold CV scheme. This enabled us to estimate the CV accuracy within a trial over time (referred to as **Session 1 CV**).

As described earlier, the dataset included also a second session of EEG measurements obtained on a different day (Session 2). Using the optimized KF-TVAR hyperparameters from the first session we extracted TV features from trials of the second session (without reapplying the KF-TVAR optimization procedure). We investigated two scenarios. In the first scenario, for each participant we predicted the motor imagery task within each trial at the time point of maximum accuracy identified in the first session. The sLDA classifier was derived at that specific time point using all the data from the first session (referred to as **Session 2 Prediction**). In the second scenario, we retrained the sLDAs through 10x1 fold CV (similarly as Session 1 CV) on the second session (referred to as **Session 2 CV**). These scenarios were both analysed to understand whether decreases in accuracy resulting from session transfer stem from the features extracted or indicate the need for recalibration of the sLDA classifier. A similar approach was also followed in Brunner et al. [7].

Statistics: For statistical testing we employed Wilcoxon's signed-rank test, along with Benjamini-Hochberg [20] correction for multiple comparisons.

RESULTS

Fig. 1 depicts the average runtime (over all participants) in seconds for the single-channel and the multi-channel optimization approaches as a function of the model order p. As the model order increases, runtime increases in both methods, with a slightly lesser impact observed for the multi-channel approach. Nevertheless,

Published by
Verlag der Technischen Universität Graz

 10.3217/978-3-99161-014-4-004

the overall runtime remains under 1 second. It's important to note, however, that runtime, is also influenced by factors such as the number of channels (here $M = 22$), sampling rate and trial length.

In Fig. 2, we present the classification accuracies (%) obtained for different scenarios using different optimization approaches (single-channel vs multi-channel optimization). Fig. 2a depicts the maximum value of the TV CV accuracy in Session 1 for all participants (Session 1 CV). In Fig. 2b, we identified, for each participant, the time point of maximum accuracy on Session 1 and utilized this time point to predict imagined movement in trials of Session 2. The KF-TVAR features were extracted from the EEG signals of Session 2 using the optimal hyperparameter sets obtained in Session 1 (Session 2 Prediction). Fig. 2b illustrates the resulting prediction accuracies. In Fig. 2c, KF-TVAR features were extracted from the EEG signals of Session 2 using the optimal hyperparameter set obtained in Session 1; however, the sLDA models were retrained using a 10x1 fold CV approach on Session 2 (Session 2 CV). The maximum accuracies acquired for each participant are depicted in Fig. 2c.

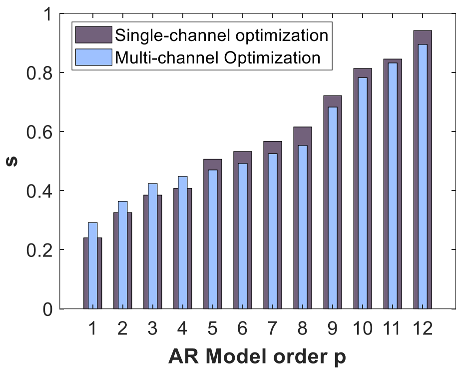

Figure 1: Average runtime (over all participants) for the single-channel and multi-channel KF-TVAR optimization approaches as a function of the AR model order p (on a 13th Gen Intel(R) Core TM i7-1355U using MEX files and a parallel pool of 10 workers). The GA was executed for 50 generations using the default *ga* Matlab settings. The upper and lower bounds for the hyperparameters were set as Q: $[0, inf]$, R: $[0, inf]$, P_0: $[0, inf]$, $\hat{\boldsymbol{a}}(0)$: $[-2,2]$.

First, we observed that CAR rereferencing led to increased accuracies (see results from sC0W0/ sC0W1/ sC1W0/ sC1W1 – significant increases ($p<0.027$) were found in Session 1 CV and Session 2 Prediction). Optimizing the initial AR coefficients $\hat{\boldsymbol{a}}(0)$, resulted into significant increases only in Session 1 CV, suggesting a possible dependence on session specific characteristics. Second, multi-channel optimization frequently resulted in higher predictive performance compared to single-channel optimization (see sC0W0/ sC0W1/ sC1W0/ sC1W1 vs vs mC1W1 and sC1W1$^+$ vs mC1W1$^+$). Third, the augmented feature set containing both the TVAR coefficients as well as the TV KF covariance trace led to significantly higher accuracies compared to considering only the TVAR coefficients (see sC0W0/ sC0W1/ sC1W0/ sC1W1 vs sC1W1$^+$ and mC1W1 vs mC1W1$^+$). Overall, mC1W1$^+$ exhibited superior performance compared to all other methods ($p<0.05$ except for the scenario Session 1 CV, where sC1W1$^+$ and mC1W1$^+$ had similar performance).

By applying session transfer from Session 1 to Session 2 (Session 2 Prediction) we observed an anticipated statistically significant decrease ($p=0.007$) in accuracy in all methods. However, after retraining the sLDA models on Session 2 while maintaining the same extracted KF-TVAR features as before, the differences were no longer statistically significant.

To provide a more holistic view of the temporal evolution of the classification results within each trial, in Fig. 3, we present the TV accuracies obtained for the various scenarios across each participant. Here, we used the proposed multi-signal mC1W1$^+$ approach. The optimal AR model orders were found to be 5, 5, 10, 7, 12, 3, 10, 4 and 2 for Participants P1, P2, P3, P4, P5, P6, P7, P8 and P9, respectively.

DISCUSSION

We presented a framework for optimal application of the KF-TVAR models on cue-based motor imagery tasks for the purposes of synchronous classification and prediction. Schlögl et al. [4] and Brunner et al. [7] have extensively examined the performance of these models and outlined a detailed process for optimizing them. Additionally, Brunner et al. [7], applied their methodology to the same motor imagery dataset analysed here. The difference of our study lies in the number of channels included in the analysis, the speed of the optimization process, as well as the methods applied for it. Brunner et al. [7] focused solely on channels C3, Cz, and C4, optimizing all relevant hyperparameters based on CV classification outcomes. In our approach, we allowed the inclusion of multiple channels, and we decoupled the KF optimization, enabling it to operate independently of the classification process (Fig. 1). Moreover, the utilization of GAs facilitates faster processing by eliminating the need to iterate through various hyperparameter values. The only hyperparameter that was selected based on CV was the AR model order p.

We decided to use single trials to optimize the KF hyperparameters in order to reduce computation runtime. We specifically selected the first trials from each class of the training set, assuming they were relatively free from significant artifacts. Our main goal during optimization was to identify the most suitable initialization hyperparameters for the KF. While the initialization phase influences tracking performance, the KF's adaptability and recursive nature, enables it to adjust to variations in the data. Thus, incorporating additional trials into the optimization process is unlikely to lead to significant changes in the final results. Regarding including single trials from all classes, the decision aimed to identify appropriate initialization hyperparameters that equally accommodate the signal characteristics of all classes, without favoring any specific class over others.

We further observed that using a single set of hyperparameters for all channels increased classification accuracies. We hypothesize that imposing uniform rate

Published by
Verlag der Technischen Universität Graz

10.3217/978-3-99161-014-4-004

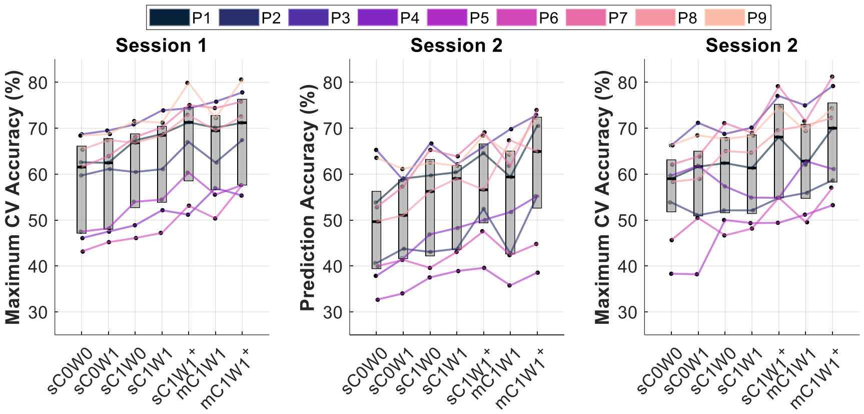

(a) (b) (c)

Figure 2: Boxplots depicting the (a) maximum CV accuracy (%) across participants on Session 1 using different KF-TVAR optimization approaches (*Session 1 CV*), (b) prediction accuracy (%) on Session 2, defined as the accuracy obtained on the time point of maximum accuracy identified in Session 1, along with the classifier derived at that specific time point (*Session 2 Prediction*) and (c) maximum CV accuracy (%) across participants on Session 2 (*Session 2 CV*). Features were extracted using the KF-TVAR hyperparameter sets obtained from Session 1. The sLDA was trained on Session 2 using a 10x1 fold CV procedure. The various colored lines represent different participants and depict the accuracy changes resulting from the application of different optimization approaches within the specific participant.

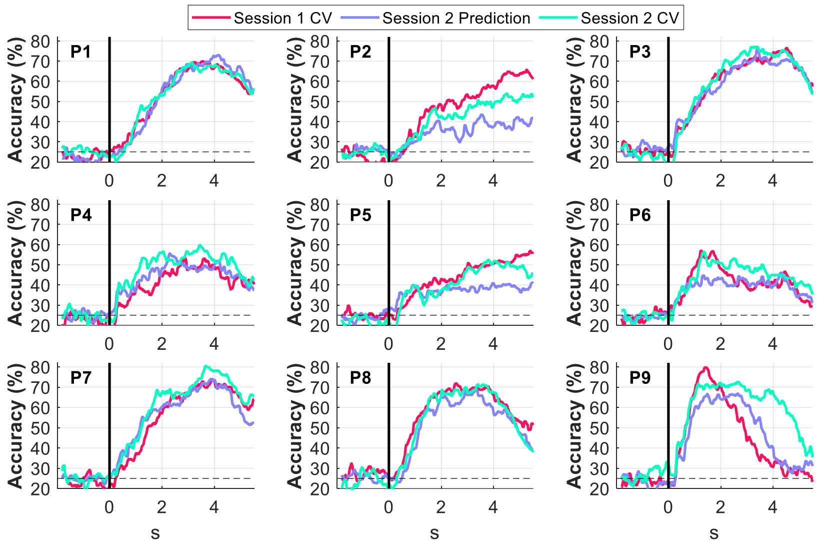

Figure 3: Temporal evolution of the accuracy (%) for each participant based on the proposed mC1W1$^+$ optimization method. The plotted curves depict the instantaneous accuracy achieved using a sample-by-sample classification approach. The black vertical line at n = 0s denotes the cue onset. *Session 1 CV* (red line) refers to the TV accuracy obtained through CV in Session 1. *Session 2 Prediction* (purple line) represents the TV accuracy estimated by extracting KF-TVAR features using the optimal hyperparameter sets obtained from Session 1, as well as the sLDA models trained on Session 1. *Session 2 CV* (cyan line) refers to the TV accuracy estimated by extracting KF-TVAR features using the hyperparameter sets obtained from Session 1, and training the sLDA models through CV on Session 2. The theoretical chance level was 25% (dashed horizontal black line at 25%).

of AR changes across all channels enhances discriminability in classification tasks and improves robustness against noisy channels. We also opted to apply the same AR model order across all channels, as assigning a unique order to each channel resulted in inferior classification performance (not shown here). Instead of relying on traditional model selection criteria such as the Akaike or Bayesian information criterion, we chose the optimal model order based on CV classification results. In [9], conventional AR model selection methods, typically applied in time-series analysis, were found inadequate for capturing discriminative EEG features related to motor imagery tasks. This implies that traditional system identification and signal analysis approaches may not always translate effectively for classification purposes. In some cases, complex tasks may necessitate a higher-order AR model to capture informative temporal patterns, whereas simpler tasks may be adequately represented by a lower-order model.

Lastly, we propose including the TV trace of the KF covariance matrix $\boldsymbol{P}(n)$ (Eq. 6) as an additional feature alongside the TVAR coefficients. This recursively estimated feature contributes positively to the classification performance. Changes in the trace of this matrix over time indicate fluctuations in the variability of the estimated coefficients. Large trace variations may correspond to periods of significant changes in the underlying EEG signals, such as transitions between

Published by
Verlag der Technischen Universität Graz

10.3217/978-3-99161-014-4-004

different states or tasks. Based on our results (Fig. 2), this feature augmentation led to significantly higher classification accuracies. In terms of signal preprocessing, we found that CAR filtering generally led to improved classification performances compared to no spatial filtering.

We observed a significant decrease in accuracy when predicting Session 2 motor imagery tasks using optimal KF-TVAR hyperparameter sets and sLDA models from Session 1 (Session 2 Prediction). This outcome was anticipated, considering Session 2 was conducted on a separate day. To determine whether this decrease stemmed from the TVAR estimation procedure or the classification algorithm, we extracted KF-TVAR features on Session 2 using the hyperparameters of Session 1 and retrained the sLDA models. The CV accuracy was found to be similar to that of Session 1, suggesting no necessity to readjust the KF-TVAR tracking, but rather the sLDA algorithm (e.g., using an adaptive sLDA).

While direct comparisons may not be feasible due to variations in CV strategies and the number of channels employed, we reference the results obtained in [7]. For scenarios Session 1 CV, Session 2 Prediction and Session 2 CV the average, across participants, 0.9 quantile of the classification accuracy was 54.28%, 39.3% and 51.12%, respectively. In contrast, the proposed mC1W1^{+} algorithm achieved 63.4%, 58.3% and 63.4%, respectively.

Our approach, initially designed for synchronous classification, can be readily adapted to asynchronous BCI applications. This can be achieved by either optimizing KF-TVAR on continuous data or by segmenting the data and extracting optimal KF-TVAR hyperparameters, as described here. Once the optimal KF-TVAR hyperparameters are determined, the TVAR coefficients can be continuously tracked. Finally, the method can be extended to other TVAR variants such as the multivariate TVAR models [7], [11]. Rather than using TVAR coefficients for classification, future work will explore AR-based root tracking techniques [13], [14], [21]. These techniques directly track the poles and zeros of the signal-generating system, capturing its dominant spectral components. This transition from AR coefficients to poles and zeros, could offer additional predictive value in discriminating various EEG tasks.

CONCLUSION

In conclusion, the methods discussed offer a robust framework for effectively applying TVAR models on BCI tasks. Future work will focus on further optimizing, speeding up and improving their application.

REFERENCES

[1] D. J. McFarland and J. R. Wolpaw, “Sensorimotor rhythm-based brain–computer interface (BCI): model order selection for autoregressive spectral analysis,” *J Neural Eng*, vol. 5, no. 2, p. 155, 2008.

[2] Y. Li, Q. Liu, S.-R. Tan, and R. H. M. Chan, “High-resolution time-frequency analysis of EEG signals using multiscale radial basis functions,” *Neurocomputing*, vol. 195, pp. 96–103, 2016.

[3] Z. G. Zhang, Y. S. Hung, and S.-C. Chan, “Local polynomial modeling of time-varying autoregressive models with application to time–frequency analysis of event-related EEG,” *IEEE Trans Biomed Eng*, vol. 58, no. 3, pp. 557–566, 2010.

[4] A. Schlögl, D. Flotzinger, and G. Pfurtscheller, “Adaptive autoregressive modeling used for single-trial EEG classification-verwendung eines Adaptiven Autoregressiven Modells für die Klassifikation von Einzeltrial-EEG-Daten,” 1997.

[5] G. Pfurtscheller, C. Neuper, A. Schlogl, and K. Lugger, “Separability of EEG signals recorded during right and left motor imagery using adaptive autoregressive parameters,” *IEEE transactions on Rehabilitation Engineering*, vol. 6, no. 3, pp. 316–325, 1998.

[6] A. Schlögl, F. Lee, H. Bischof, and G. Pfurtscheller, “Characterization of four-class motor imagery EEG data for the BCI-competition 2005,” *J Neural Eng*, vol. 2, no. 4, p. L14, 2005.

[7] C. Brunner, M. Billinger, C. Vidaurre, and C. Neuper, “A comparison of univariate, vector, bilinear autoregressive, and band power features for brain–computer interfaces,” *Med Biol Eng Comput*, vol. 49, pp. 1337–1346, 2011.

[8] H. Nai-Jen and R. Palaniappan, “Classification of mental tasks using fixed and adaptive autoregressive models of EEG signals,” in *The 26th Annual International Conference of the IEEE Engineering in Medicine and Biology Society*, 2004, pp. 507–510.

[9] A. Atyabi, F. Shic, and A. Naples, “Mixture of autoregressive modeling orders and its implication on single trial EEG classification,” *Expert Syst Appl*, vol. 65, pp. 164–180, 2016.

[10] B. Graimann, J. E. Huggins, A. Schlogl, S. P. Levine, and G. Pfurtscheller, “Detection of movement-related patterns in ongoing single-channel electrocorticogram,” *IEEE Transactions on neural systems and rehabilitation engineering*, vol. 11, no. 3, pp. 276–281, 2003.

[11] L. Astolfi *et al.*, “Tracking the time-varying cortical connectivity patterns by adaptive multivariate estimators,” *IEEE Trans Biomed Eng*, vol. 55, no. 3, pp. 902–913, 2008.

[12] K. Kostoglou, A. D. Robertson, B. MacIntosh, and G. D. Mitsis, “A novel framework for estimating time-varying multivariate autoregressive models and application to cardiovascular responses to acute exercise,” *IEEE Trans Biomed Eng*, 2019.

[13] K. Kostoglou and M. Lunglmayr, “Root tracking using time-varying autoregressive moving average models and sigma-point Kalman filters,” *EURASIP J Adv Signal Process*, vol. 2020, no. 1, p. 6, Dec. 2020, doi: 10.1186/s13634-020-00666-7.

[14] L. T. Mainardi, A. M. Bianchi, G. Baselli, and S. Cerutti, “Pole-Tracking Algorithms for the Extraction of Time-Variant Heart Rate Variability Spectral Parameters,” *IEEE Trans Biomed Eng*, vol. 42, no. 3, pp. 250–259, 1995, doi: 10.1109/10.364511.

[15] M. Tangermann *et al.*, “Review of the BCI competition IV,” *Front Neurosci*, p. 55, 2012.

[16] L. Ljung and T. Söderström, *Theory and practice of recursive identification*. MIT press, 1983.

[17] M. F. Pagnotta and G. Plomp, “Time-varying MVAR algorithms for directed connectivity analysis: Critical comparison in simulations and benchmark EEG data,” *PLoS One*, vol. 13, no. 6, p. e0198846, 2018.

[18] K. Kostoglou and G. D. Mitsis, “Modelling of multiple-input, time-varying systems with recursively estimated basis expansions,” *Signal Processing*, 2018, doi: S0165168418303207.

[19] Olivier Ledoit, “covShrinkage (https://github.com/oledoit/covShrinkage/releases/tag/1.1.0), GitHub.”

[20] Y. Benjamini and Y. Hochberg, “Controlling the false discovery rate: a practical and powerful approach to multiple testing,” *Journal of the Royal statistical society: series B (Methodological)*, vol. 57, no. 1, pp. 289–300, 1995.

[21] G. Müller-Putz, M. Crell, J. Egger, P. Suwandjieff, and K. Kostoglou, “Towards Implantable Brain-Computer Interface for Communication in Locked-In Syndrome patients: An introduction to INTRECOM,” in *Current Directions in Biomedical Engineering*, 2023, pp. 1–4.

Published by
Verlag der Technischen Universität Graz